JAAS

ROYAL SOCIETY OF CHEMISTRY

PAPER

View Article Online
View Journal

Cite this: DOI: 10.1039/d6ja00014b

A direct solid sampling approach for fluorine determination *via* ETV/ICP-QQQ-MS

Vera M. Scharek, Heike Traub and Björn Meermann *

Organic fluorine sum parameters are used to detect F-containing pollutants, *e.g.*, per- and polyfluoroalkyl substances (PFASs), in the environment, within materials, or for monitoring technical processes, *e.g.*, thermal decomposition of PFAS during municipal waste incineration. However, established approaches determining the extractable organic and adsorbable organic fluorine content (EOC and AOC) require laborious and error-prone sample preparation. We report a solid sampling-electrothermal vaporization (ETV) method for direct fluorine measurement based on the formation of $[^{138}Ba^{19}F]^+$ with an inductively coupled plasma-triple quadrupole-mass spectrometer (ICP-QQQ-MS). Method development involved the instrumental setup for Ba introduction and fluorine-specific tuning of lens and collision-reaction cell (CRC) parameters. An inorganic fluorine fraction was detected in a cyclonic dust sample from a municipal waste incineration plant as a peak above a broad background signal. The content was estimated through standard addition using a NaF solution to 2300 μg g^{-1}. With a limit of detection (LOD) of 130 μg g^{-1}, which was below the reported value for an electrothermal vaporization/inductively coupled plasma-mass spectrometry (ETV/ICP-MS) approach, acquiring $[^{19}F]^+$. The method's potential for fractionation analysis was demonstrated by analyzing polytetrafluoroethylene (PTFE) powder.

Received 9th January 2026
Accepted 26th February 2026

DOI: 10.1039/d6ja00014b

rsc.li/jaas

Introduction

Fluorine is ubiquitously distributed on the earth and occurs in the form of fluoride anions, *e.g.*, in seawater,[1] and as hydroxy silicates and apatite (>1 wt% in fluorine-rich rocks) in the lithosphere.[2] While the occurrence of natural organofluorides was reported, *e.g.*, fluoroacetate in plant extracts,[3] most fluorinated organic substances are of anthropogenic origin. Due to the high polarity and bond energy of the C–F bond (105.4 kcal mol^{-1}), organofluorine compounds exhibit alternated physicochemical properties and enhanced thermodynamic stability.[4] Consequently, these compounds are found in a wide range of industrial applications, including herbicides and pharmaceuticals with enhanced drug efficiency,[5] as well as fluoropolymers for waterproof clothing, non-stick surfaces in cookware, and in solar and fuel cells.[2,5] Among organofluorines, the emerging substance class of per- and polyfluoroalkyl substances (PFASs) has gained recent attention.

PFASs are found in everyday products, including food packaging, cookware, textiles, ski wax, as well as building and automotive materials,[6] due to their hydro- and oleophobic properties. However, the highly stable compounds are suspected to have adverse health effects.[7] Through the risk of liquid leachates, PFAS-containing waste in landfills poses a time-delayed source.[7] The remineralization of PFAS is regarded as the only permanent solution, demanding destructive processes.[7] During thermal waste treatment, solid reaction products such as coke, polymeric material, and mineralized fluorine are formed alongside gaseous products, *e.g.*, CO_2, CO, HF.[6] Thereby, volatile and new PFASs are generated through incomplete destruction and can be emitted into the atmosphere.[6,7]

To detect the release of fluorine-containing compounds into the environment and investigate the fate of PFASs, a comprehensive fluorine analysis is necessary. So far, no single robust quantitative method is available.[6] In solid residues, PFAS analysis is possible after extraction, purification, and enrichment steps. However, targeted approaches are limited by the large variety of the substance class (>19 000 listed chemicals),[8] which is further diversified by degradation products. Non-specific mass balance approaches encompass the determination of organic fluorine sum parameters in extracts of solid samples.[9,10] Thereby, the extractable or adsorbable organic fluorine (EOF/AOF) content after solid-phase extraction and adsorption at activated carbon, respectively, is quantified by combustion ion chromatography (CIC). For solid analysis, these parameters strongly depend on the extraction medium.[10] Detection *via* fluoride ion-selective electrodes (F-ISE) in combination with sample combustion is used for screening high-fluoride systems.[11] Hence, a direct solid sampling approach for fluorine fractionation would be beneficial. K-edge X-ray absorption near-edge structure spectroscopy has been applied for the

Federal Institute for Materials Research and Testing (BAM), Division 1.1 – Inorganic Trace Analysis (ITALab), Richard-Willstätter-Straße 11, Berlin 12489, Germany. E-mail: bjoern.meermann@bam.de

speciation of fluorine compounds in soil.[10] However, the surface technique yields (semi-) quantitative results. While nuclear activation techniques, *e.g.*, instrumental neutron activation analysis, are suitable for fluorine screening, fractionation analysis is not feasible.[12]

Recently, laser-ablation coupled to inductively coupled plasma-mass spectrometry (LA/ICP-QQQ-MS) has been reported for fluorine mapping using the polyatomic ion formation of BaF.[13] Fluorine detection with ICP-MS is challenging due to the high ionization potential of fluorine (17.42 eV) and spectral interferences from double-charged $[^{38}Ar]^{2+}$ and other polyatomic species, *e.g.*, $[^{1}H^{18}O]^{+}$. Attempts to resolve the monoisotopic $[^{19}F]^{+}$ with a sector-field ICP-MS and electrothermal vaporization (ETV) were successful but yielded low sensitivities (μg g^{-1} to percentage level).[14,15] The determination of $[^{19}F]^{-}$ with an ICP-MS in negative-mode was reported by Vickers *et al.* and Raab *et al.*.[16,17] However, instrumental modifications are required to detect negatively charged ions. A method using a plasma-assisted reaction chemical ionization was developed by Lesniewski *et al.*.[18] Thereby, neutral species formed in the plasma are ionized in an afterglow reaction tube by reacting with ions. Measuring $[BaF]^{+}$ with an ionization potential of 4.70 eV was first described in a feasibility study by Yamada and enabled the determination of fluorine in sub-μg g^{-1} levels.[19] The reduction of Ba-derived interferences was achieved with collision reaction cell (CRC) technology, utilizing O_2 (on-mass) and NH_3/He in mass-shift mode. Jamari *et al.* applied s-lenses with inverted extraction voltages for the detection of fluorine-containing compounds in water with an optimal signal-to-background ratio at energetic CRC conditions (−60 V OctP-bias, 0.75 mL min^{-1} O_2).[20] Plasma conditions and sampling position were found to be crucial for $[BaF]^{+}$ formation and sampling, showing a high matrix dependency.[20,21] The BaF approach has been used for several applications, *e.g.*, speciation with chromatographic coupling[22] and single particle measurements of polytetrafluorethylene (PTFE) particles.[23,24] To the authors' knowledge, the method has not been adapted to ETV/ICP-QQQ-MS, whose speciation and fractionation capability has been shown for Hg and Sn, respectively.[25,26]

This work aimed to develop an ETV/ICP-QQQ-MS method for the detection of fluorine as $[BaF]^{+}$, encompassing the instrumental setup and tuning of the solid sampling introduction system. To demonstrate the methods' applicability for the direct analysis of solid samples, we analyzed a dust sample from a field campaign on the behavior of PFAS during thermal waste treatment. The quantification of the (total) fluorine content was carried out *via* standard addition as a proof-of-concept approach and compared to F-ISE measurements of the sample after combustion. Furthermore, we investigated the fractionation potential of ETV for determining fluorine sum parameters.

Experimental

Chemicals

Fluoride standard solution (1000 mg L^{-1} F from NaF in H_2O) and barium standard for ICP (1 g L^{-1} Ba in nitric acid) were purchased from Merck (Darmstadt, Germany). Purified water from a Milli-Q water purification system (Merck Millipore, France) was used. Nitric acid (HNO_3, 65% (w/w)) from Th. Geyer (Renningen, Germany) was sub-boiled prior to use. Fluorine-specific tuning was performed using trifluoromethane (GHC, Hamburg, Germany). PTFE nanopowder (99.9%) was obtained from Nanografi Nano Technology (Ankara, Turkey).

Cyclonic dust sample

The cyclonic dust sample was obtained during a field campaign within the framework of the German Federal Environmental Agency's departmental research plan on the subject "Outward transfer of pollutants from material circulation through thermic procedures" in February 2025. To investigate processes on an industrial scale, test series were conducted at the municipal waste incineration plant of the joint venture power-generating plant in Schweinfurt (Gemeinschaftskraftwerk Schweinfurt GmbH, GKS).

Instrumentation

An ETV system ETV-4000d, equipped with an autosampler AD30 (Spectral Systems, Fürstenfeldbruck, Germany) was used as a solid sampling unit for an 8900 triple quadrupole ICP-MS (Agilent, Waldbronn, Germany). S-lenses with nickel cones, and a quartz torch with a 2.5 mm inner diameter were used (Agilent, Waldbronn, Germany). Lens and CRC parameters were tuned with CHF_3 through the ETV reaction gas inlet. Table 1 includes typical parameter values. Pyrolytically coated sample boats and tubes (Size "maxi", Spectral Systems, Fürstenfeldbruck, Germany) were utilized. The temperature reading of the internal ETV pyrometer was adjusted to an external pyrometer PKL 38 AF 1 (KELLER HCW GmbH, Ibbenbüren, Germany) prior to each measurement day. The ETV system was operated with carrier and bypass gas flows of 0.142 L min^{-1} and 0.420 L min^{-1} argon, respectively. For mixing of the barium solution (100 mg L^{-1}, prepared in diluted nitric acid) with the ETV sample gas flow, an inlet system developed for the on-line introduction of standard solutions was used.[26] The inlet system is based on a modified cyclonic quartz spray chamber (Thermo Fisher Scientific, Bremen, Germany) equipped with a low-flow nebulizer (X175, Burgener Research Inc., Mississauga, Ontario, Canada) operated at 7.5 μL min^{-1}. Operating conditions are listed in Table 1. $[^{138}Ba^{19}F]^{+}$ and $[^{40}Ar^{40}Ar]^{+}$, as a plasma indicator,[27] were measured on-mass. To observe fluctuations in the Ba proliferation, $[^{135}Ba]^{+}$ were acquired with a mass shift to $[^{135}Ba^{16}O^{16}O]^{+}$ (*m*/*z* 167).

Results and discussion

Method development

Measuring fluorine as $[BaF]^{+}$ is an established approach for ICP-QQQ-MS analysis.[13,20,22–24] However, transferring liquid analysis setups to solid sample introduction requires modification of (i) the introduction of Ba into the plasma along with the sample, and (ii) adaptation of the tuning procedure. Liquid analysis commonly involves the on-line introduction of the barium

Table 1 Operating conditions of the ETV/ICP-MS system[a]

ICP parameter	Value
ICP-MS instrument	8900 triple quadrupole
Ion optics	S-lenses, 200.0 V (extract 1)[a], 3.0 V (extract 2)[a], 9.2 V (deflect)[a]
Cones	Ni sampler and skimmer cone
Plasma power (W)	1500
ICP gas flows (L min^{-1})	0.90 (auxiliary gas), 15.0 (plasma gas)
Nebulizer gas pressure (psi)	65, equaling an argon gas flow of 1.04 L min^{-1}
Sampling depth (mm)	3.0

CRC mode	Value
Reaction gas	O_2
Reaction gas flow (mL min^{-1})	0.30
Octopole bias (V)	−5.0
Energy discrimination (V)	−10.0

ETV parameter	Value
ETV system	ETV-4000d equipped with autosampler AD30
Sample boats and tubes	Pyrolytically coated graphite, size "maxi"
ETV gas flows (L min^{-1})	0.142 (carrier gas), 0.420 (bypass gas)

Acquisition parameter	Value
Acquisition mode	Time-resolved analysis
Scan type	MS/MS
Isotopes monitored	$[^{138}Ba^{19}F]^+$, $[^{40}Ar^{40}Ar]^+$ (both on-mass), $[^{135}Ba]^+ \rightarrow [^{135}Ba^{16}O^{16}O]^+$
Integration time per mass	30 ms

[a] Typical value after tuning with CHF_3.

solution through a T-piece.[20,23] With ETV, it is possible to add barium directly to the sample into the graphite boat. In our approach, we opted for on-line addition using a separate nebulization system, as the vaporization temperatures of fluorine-containing components and ionic barium are presumably different from each other. The aerosol was generated *via* a low-flow nebulizer, reducing the water intake into the plasma, which was found favorable for $[BaF]^+$ analysis by Clases *et al.*.[13]

Fluorine-specific tuning of the instrument parameter is essential for optimal $[BaF]^+$ sampling from the plasma.[13,20] In conventional ICP-MS, plasma parameters are optimized based on example elements. However, the polyatomic formation presumably takes place in a small plasma zone after the maximum ion density of $[Ba]^+/[Ba]^{2+}$.[21] To avoid the laborious comparison of transient signals from the vaporization of fluorine standards, we utilized the reaction gas inlet of the ETV system to generate a continuous fluorine flow to the ICP. A dwell time of 30 ms was selected as a compromise between signal intensity and acquiring sufficient data points for peak evaluation. Jamari *et al.* reported a narrow optimum for nebulizer and make-up gas flows.[20] In our setup, the gas flows of the sample introduction system were determined by technical requirements, *e.g.*, from ETV. We adjusted the sampling position to a hot plasma region close to the load coil (3.0 mm), similar to that reported for LA-measurements.[13]

In standard mode, the 8900 triple quadrupole is operated using a so-called "x-lens", which deflects the ion beam off-axis to the sampling interface axis to remove photons and non-charged species. However, polyatoms have less kinetic energy and tend to diffuse at the edge of the ion beam, reducing their transmission. Following previous work, a s-lens was used for increased ion transmission by focusing the ion beam on a straight path.[13,20,23] Optimal lens parameters were comparable to reported values.[13] Due to the absence of water in the system, little formation of the isobaric interference $[^{138}Ba^{18}O^1H]^+$ was expected. Additionally, a constant background signal would be

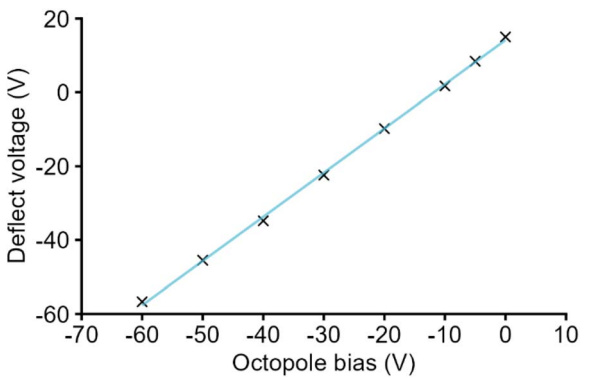

Fig. 1 Deflect voltage as a function of the octopole bias. The blue line shows the linear correlation.

separable from peak signals through treatment of the time-resolved analysis data. Hence, we aimed to tune the CRC conditions for maximum sensitivity with less energetic CRC conditions in O_2 mode. The highest signal intensities were observed for an octopole bias of −5.0 V. Thereby, a linear correlation between the collision energy and the deflect lens voltage was found (Fig. 1). Deflect lens guides ions into the CRC, where a more negative octopole bias increases the collision energy. Consequently, the ion inlet into the cell appears to influence the CRC processes depending on the applied acceleration energy.

Analysis of solid samples

By gradually increasing the temperature of the furnace, matrix and sample components of different boiling points can be separated *via* ETV to prevent signal suppression through plasma loading. Fluorine detection as $[BaF]^+$ is especially sensitive to plasma alteration, since the polyatomic formation occurs in a small temperature zone in the plasma. Non-spectral interferences can be observed by monitoring the argon dimer $[^{40}Ar^{40}Ar]^+$.[26,27] For *m*/*z* 80, the ETV time scan of the dust sample showed two peaks at ∼125 s and ∼170 s, equaling furnace temperatures of about 900 °C and 1350 °C, respectively (Fig. S1 in the SI). Due to their distinct shapes, the peaks could be ascribed to the vaporization of selenium components present in the sample rather than plasma effects. Barium was detected *via* *m*/*z* (135 → 167). Presuming a constant proliferation, detecting $[^{135}Ba]^+$ as $[^{135}Ba^{16}O^{16}O]^+$ could be used as an indicator for non-spectral interferences, considering the plasma reaction of Ba to BaF.

The ETV time scan of the dust sample is depicted in Fig. 2. Until an ETV temperature of about 750 °C (∼110 s), constant signal curves were observed for $[^{138}Ba^{19}F]^+$ and $[^{135}Ba^{16}O^{16}O]^+$. A moderate baseline level of 10^4 cts was acquired for *m*/*z* 157, coinciding with blank measurements. An example time scan of an empty graphite boat is provided in the SI (Fig. S2). Starting at 110 s, *m*/*z* 157 and 167 signals decreased until a rebound at 175 s (∼1400 °C), indicating the vaporization of matrix components. After the signal increase, the Ba signal remains steady except for small variations. With approximately 2×10^4 cts, the $[^{135}Ba^{16}O^{16}O]^+$ signal intensity stays below the value of the first part of the ETV program (0–120 s), probably due to signal suppression through ongoing matrix vaporization.

The $[BaF]^+$ signal shows a small peak at 180 s (∼1450 °C). However, the peak did not appear in further measurements with standard addition (Fig. 3A in the following section) and could be caused by plasma fluctuation. At approximately 1800 °C (∼215 s), a steep signal increase was detected, denoting the vaporization of presumably inorganic fluorine-containing compounds (FCCs). The intensity of *m*/*z* 157 remains at a high level (>1.1×10^5 cts) until the end of the temperature program, accompanied by the cooling of the furnace. Although no noticeable sample residue was observed in the graphite boats, incomplete fluorine release from minerals, *e.g.*, F incorporated in quartz (melting point: 1610 °C, boiling point: > 2230 °C), could cause this finding. The use of a reaction gas for complete sample vaporization was not feasible since commonly F-containing Freon gases are utilized for this purpose. In the time scan section 215 – 306 s, the shape of the $[BaF]^+$ signal appeared irregular. However, a peak was recognized at ∼240 s (2040 °C), indicating the detection of an F-fraction with different vaporization behavior. The vaporization of PFAS was expected at temperatures below 250 °C, while the release of surface-mediated decomposition products was found in experiments with activated carbon up to 900 °C.[28] Hence, the peak was not directly associated with PFAS detection.

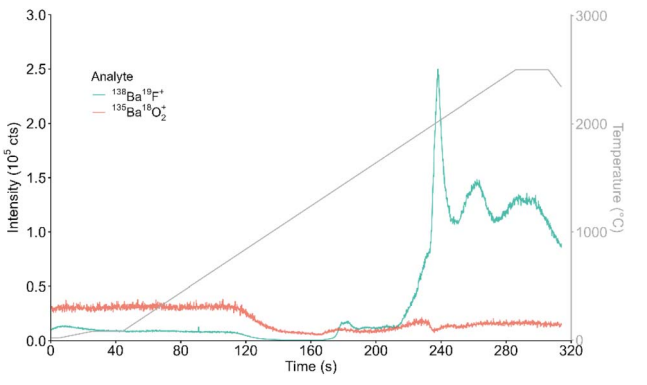

Fig. 2 ETV/ICP-QQQ-MS time scan of cyclonic dust (without standard addition) acquired in MS/MS scan mode. The CRC was pressured with an oxygen gas flow of 0.03 mL min^{-1}. The ETV temperature program is shown in grey.

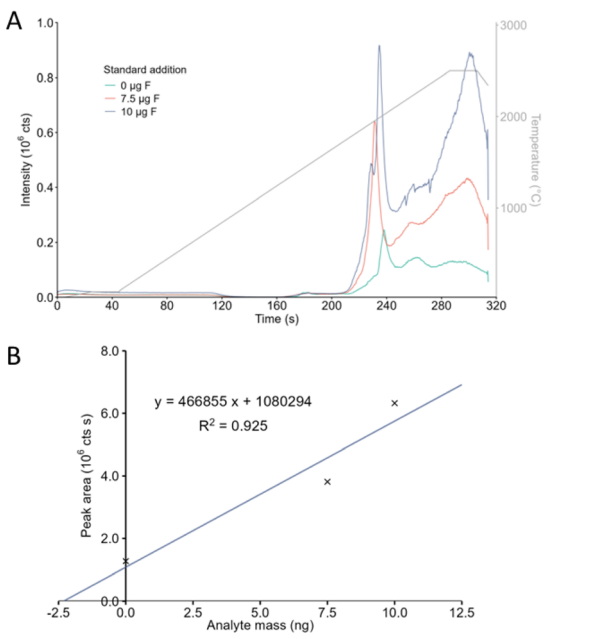

Fig. 3 (A): *m*/*z* 157 ETV time scans of dust samples without added fluoride standard and spiked with 7.5 and 10 µg inorganic fluorine (as NaF solution). The CRC was pressurized with an oxygen gas flow of 0.03 mL min^{-1}. The temperature program is shown in grey. (B): Peak areas as a function of the added fluoride mass for determining the content of an inorganic fluorine fraction in the dust sample (standard addition approach). The analyte amount in the sample was obtained as the intercept of the linear fit with the *x*-axis.

Calibration *via* standard addition

Calibration strategies for ETV encompass external calibration,[29] standard addition,[30] and isotope dilution mass spectrometry.[25,26,31] In our proof-of-concept approach, we attempted to calibrate using a standard addition approach as the detection of $[^{138}Ba^{19}F]^+$ is highly sensitive to plasma changes, which were indicated by signal suppression of *m*/*z* 80 and *m*/*z* (135 → 167) in the F-peak time window (215–250 s, Fig. S1). Isotope dilution mass spectrometry is not feasible as fluorine is monoisotopic. For external calibration, no suitable reference material was available. Adding increasing amounts of inorganic fluorine as an aqueous sodium fluoride solution resulted in a signal enhancement of *m*/*z* 157 between 215–306 s (Fig. 3A). With a boiling point of 1704 °C, we expected NaF to vaporize within the ETV temperature program. Hence, the increase in the *m*/*z* 157 signal intensity presumably originates from the build-up of refractory matrix components, *e.g.*, in cooler parts of the ETV graphite tube. Additionally, the ETV time scans showed an intensification of the peak at *circa* 230–240 s. The peak was assigned to an inorganic fluorine fraction based on the following considerations: (i) The furnace temperature at the peak detection time was in approximate accordance with the boiling point of alkali fluorides. Deviations could be explained through analyte–matrix interactions, the heating delay of the ETV system, and the transport time to the ICP. (ii) The reproducible peak shape suggests a faster vaporization in comparison to more refractory FCCs, which were detected as a broad signal with a duration of more than 90 s. Thus, the *m*/*z* 157 signal peak suggests the presence of adhesive FCCs that are not incorporated into a refractory mineral phase. (iii) A linear correlation of peak area and added fluoride standard (standard addition approach) was found (Fig. 3B), verifying the assignment to (adherend) fluorides. The inorganic FCCs could (partly) originate from PFAS mineralized during the waste incineration.

A linear three-point calibration curve (R^2 = 0.925) was established using the baseline-corrected areas of the *m*/*z* 157 peak at 230–240 s and is depicted in Fig. 3B. The fluorine amount was estimated through extrapolation to the intercept of the *x*-axis to 2300 μg g^{-1}. F-ISE measurements after combustion yielded the approximate threefold total fluorine amount (7200 μg g^{-1}). The difference in the amount is explainable through partial integration of the $[^{138}Ba^{19}F]^+$ signal. However, integrating the $[^{138}Ba^{19}F]^+$ signal over the whole range (215–320 s, 11.2 × 10^6 cts s) amounts to ten times the peak area obtained through our approach. This could be attributed to sample inhomogeneity or incomplete combustion of the sample. A temperature of 1050 °C or similar in the combustion unit may not decompose high-melting inorganic fluorine.[9] The addition of WO_3 is reported to function as a flux and could be used as a modifier for ETV measurements.[10] However, the original vaporization characteristics of the analyte might get lost through the utilization of a modifier.

The limit of detection and quantification (LOD and LOQ) were calculated as three and ten times the standard deviation of blank signals divided by the slope of the calibration curve to 0.13 and 0.42 μg, respectively (130 and 420 μg g^{-1} for a theoretical sample mass of 1 mg). The estimated limits were approximately two times lower than a previously published LOD of 0.29 μg for the direct measurement of $[^{19}F]^+$ *via* ETV/ICP-MS.[15] Using the BaF approach, Jamari *et al.* reported a ~100-fold improvement of the LOD for F in deionized water compared to $[^{19}F]^+$ HR-ICP-MS measurements (5070 mg L^{-1}).[14,20] A LOD of 54 mg L^{-1} was reported for fluorine measurement with ICP-MS in negative-mode.[17] The focus of our proof-of-concept study was on the method development using ETV/ICP-QQQ-MS for $[^{138}Ba^{19}F]^+$ detection and investigating the fractionation capability of ETV for FCCs in a real-world sample. However, a 50-times lower LOD (2.7 μg g^{-1}) was described for LA/ICP-QQQ-MS, showing the method's potential in combination with solid sampling approaches.[13] For solid CIC measurements, a LOD at sub-ng level (0.5 ng) was reported with the additional advantage of a higher sample capacity (40 mg) compared to ETV/ICP-QQQ-MS.[10] Depending on the ETV program, the combustion time for CIC measurements is comparable.[12] However, the IC run time is typically longer, *e.g.*, 22 min.[10] Additional time is needed for sample preparation when determining the EOF (>1 h/sample) since direct CIC analysis would only yield the TF.[10,12] Hence, the main benefits of using ETV/ICP-QQQ-MS are to obtain information on sum parameters through fractionation that would otherwise require time-consuming and error-prone sample preparation.

PTFE sample

Residual organic fluorine in the cyclonic dust sample could indicate an incomplete destruction of PFAS and other organic FCCs during the waste incineration procedure. The separation of an organic fluorine fraction could serve as an alternative to established sum parameters, such as EOF and AOF. However, an EOF below the LOD of the ETV/ICP-QQQ-MS method (510 ppb) was determined by CIC, and we did not observe additional peaks in the *m*/*z* 157 time scan. To further investigate the fractionation potential of ETV, PTFE powder was analyzed using the same temperature program as for the dust sample. The $[^{138}Ba^{19}F]^+$ time scan is shown in Fig. 4. A peak at ~110 s, corresponding to a furnace temperature of 740 °C, was assigned to

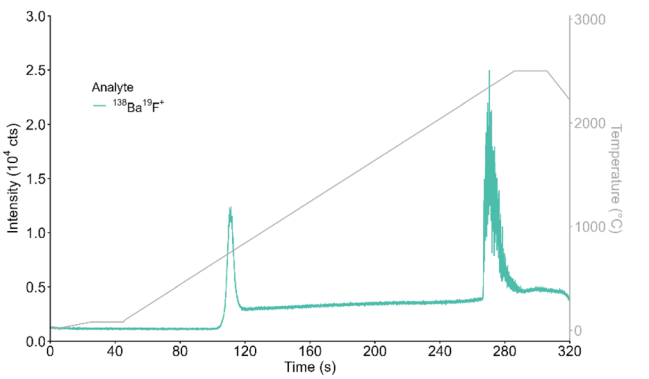

Fig. 4 *m*/*z* 157 ETV time scans of pure PTFE powder (*m* = 0.17 mg F). The CRC was pressurized with an oxygen gas flow of 0.03 mL min^{-1}. The ETV temperature program is shown in grey.

the release of volatile FCCs through the pyrolysis of PTFE and is in agreement with the literature (500–650 °C).[28] After the peak, the $[^{138}Ba^{19}F]^+$ signal remains at an elevated level (~3 times the baseline), indicating a successive pyrolysis. At an ETV temperature of 2400 °C, a second, noisier, tailing peak was observed, which could originate from an additional pyrolysis step. However, little is reported in the literature for this temperature range. Condensation of FCCs in cooler parts of the system released at higher temperatures could cause the $[^{138}Ba^{19}F]^+$ signal.

Concludingly, separating PTFE (110 s) and inorganic fluorine (230 s) peaks *via* the applied ETV temperature program would be feasible, and could presumably be transferred to the analysis of other organic FCCs. However, incomplete vaporization, memory effects, and analyte–matrix interaction, as described for the fractionation analysis of organotin compounds in sediment, must be considered.[26] Thus, further careful method development and validation is required.

Conclusions

In this work, we developed an ETV/ICP-QQQ-MS method for the direct fluorine determination of solid samples measuring $[^{138}Ba^{19}F]^+$. Mixing of the barium solution for polyatomic formation was accomplished in a modified cyclonic spray chamber using a low-flow nebulizer. CHF_3 was utilized as an F-source for the tuning of lens and CRC parameters. As a proof-of-concept, a cyclonic dust sample from a municipal waste incineration study was analyzed with an ETV temperature ramp from 100 to 2500 °C (10 K s^{-1}). An inorganic fluorine fraction was identified and quantified through standard addition with a NaF solution. To further investigate the potential of separating an organic F-fraction, the vaporization behavior of PTFE powder was characterized.

We demonstrated the feasibility of determining the fluorine fraction in a dust sample without prior sample preparation. The decrease of the $[^{138}Ba^{19}F]^+$ signal after the end of the temperature program was assigned to incomplete vaporization, presumably due to fluorine incorporated into a refractory mineral phase. However, a peak at ~240 s (2040 °C) was verified as an inorganic fluorine fraction that could originate from adherent alkali fluorides and was estimated to 2300 μg g^{-1}. An approximate threefold total fluorine content was yielded by F-ISE measurement after combustion. From the total $[^{138}Ba^{19}F]^+$ signal, an even higher actual fluorine content of the sample was anticipated. LOD and LOQ were determined at the upper μg g^{-1} level (130 and 420 μg g^{-1}, respectively). However, reported literature values of BaF-approaches suggest that significantly lower limits are achievable through further method optimization. Pure PTFE powder was analyzed, since an organic F-fraction was not identifiable in the dust sample. A $[^{138}Ba^{19}F]^+$ peak at 740 °C (110 s) indicated the PTFE pyrolysis and would be separable from inorganic fluorine. Due to an elevated background level and a second peak at higher furnace temperatures, further method development is required for fractionation analysis.

As pointed out, further work is necessary for fractionation analysis of real-world samples. However, we could show that ETV/ICP-QQQ-MS in combination with the BaF-approach has potential as an alternative to the established fluorine sum parameter methods. By the measurement of m/z 80 and (135 → 167), we could demonstrate the method's suitability for a multi-element approach. By this, the analysis time could be reduced and the coherence between different element fractionation recognized.

Author contributions

Vera Scharek: writing original draft, conceptualization, data curation, investigation. Heike Traub: review and editing, conceptualization, supervision. Björn Meermann: review and editing, conceptualization, funding acquisition, supervision.

Conflicts of interest

The authors declare no competing interests.

Data availability

All data will be made available upon request to the corresponding author.

Supplementary information (SI) is available. See DOI: https://doi.org/10.1039/d6ja00014b.

Acknowledgements

The authors thank Daniel Wohter from the RWTH Aachen University for providing the dust sample and Dr Matthias Schmitt (BASF) for the F-ISE reference measurement.

References

1 Y. Miyake, N. Yamashita, P. Rostkowski, M. K. So, S. Taniyasu, P. K. S. Lam and K. Kannan, *J. Chromatogr. A*, 2007, **1143**, 98–104.
2 R. Fuge, *Appl. Geochem.*, 2019, **100**, 393–406.
3 M. L. Baron, C. M. Bothroyd, G. I. Rogers, A. Staffa and I. D. Rae, *Phytochemistry*, 1987, **26**, 2293–2295.
4 D. O'Hagan, *Chem. Soc. Rev.*, 2008, **37**, 308–319.
5 A. Harsanyi and G. Sandford, *Green Chem.*, 2015, **17**, 2081–2086.
6 J. L. Wang, Z. H. Lin, X. X. He, M. R. Song, P. Westerhoff, K. Doudrick and D. Hanigan, *Environ. Sci. Technol.*, 2022, **56**, 5355–5370.
7 M. G. Evich, M. J. B. Davis, J. P. McCord, B. Acrey, J. A. Awkerman, D. R. U. Knappe, A. B. Lindstrom, T. F. Speth, C. Tebes-Stevens, M. J. Strynar, Z. Y. Wang, E. J. Weber, W. M. Henderson and J. W. Washington, *Science*, 2022, **375**, 512.
8 U. S. E. P. Agency, *List of PFAS chemicals without explicit structures*, https://comptox.epa.gov/dashboard/chemical-lists/PFASDEV3, (accessed 11/14/2025).

9 L. Gehrenkemper, F. Simon, P. Roesch, E. Fischer, M. von der Au, J. Pfeifer, A. Cossmer, P. Wittwer, C. Vogel, F. G. Simon and B. Meermann, *Anal. Bioanal. Chem.*, 2021, **413**, 103–115.
10 P. Roesch, C. Vogel, T. Huthwelker, P. Wittwer and F. G. Simon, *Environ. Sci. Pollut. Res.*, 2022, **29**, 26889–26899.
11 M. Ignacio, G. W. Curtzwiler, M. R. Early, K. M. Updegraff and K. L. Vorst, *Methods Protoc.*, 2023, **6**(1), 10.
12 C. P. Shelor, C. Warren, C. V. Odinaka and K. Dumre, *J. Sep. Sci.*, 2024, **47**, 2400235.
13 D. Clases, R. G. de Vega, J. Parnell and J. Feldmann, *J. Anal. At. Spectrom.*, 2023, **38**, 1661–1667.
14 X. D. Bu, T. B. Wang and G. Hall, *J. Anal. At. Spectrom.*, 2003, **18**, 1443–1451.
15 Y. Okamoto, *J. Anal. At. Spectrom.*, 2001, **16**, 539–541.
16 G. H. Vickers, D. A. Wilson and G. M. Hieftje, *Anal. Chem.*, 1988, **60**, 1808–1812.
17 A. Raab, H. Badiei and J. Feldmann, *J. Anal. At. Spectrom.*, 2025, **40**, 1689–1699.
18 J. E. Lesniewski, K. Y. Zheng, P. Lecchi, D. Dain and K. Jorabchi, *Anal. Chem.*, 2019, **91**, 3773–3777.
19 N. Yamada, *Agil. 8800 ICP-QQQ Appl. Handb., Agilent Tecnologies*, 2013, 33–34.
20 N. L. A. Jamari, J. F. Dohmann, A. Raab, E. M. Krupp and J. Feldmann, *J. Anal. At. Spectrom.*, 2017, **32**, 942–950.
21 N. L. A. Jamari, A. Behrens, A. Raab, E. M. Krupp and J. Feldmann, *J. Anal. At. Spectrom.*, 2018, **33**, 1304–1309.
22 N. L. A. Jamari, J. F. Dohmann, A. Raab, E. M. Krupp and J. Feldmann, *Anal. Chim. Acta*, 2019, **1053**, 22–31.
23 R. G. de Vega, T. T. Moro, B. Grüner, T. D. Maranhao, M. J. Huber, N. P. Ivleva, E. Skrzypek, J. Feldmann and D. Clases, *J. Anal. At. Spectrom.*, 2024, **39**, 2030–2037.
24 F. Gelman, M. Muszynska, J. Karasinski, O. Lev and L. Halicz, *J. Anal. At. Spectrom.*, 2022, **37**, 2282–2285.
25 I. Gelaude, R. Dams, M. Resano, F. Vanhaecke and L. Moens, *Anal. Chem.*, 2002, **74**, 3833–3842.
26 V. M. Scharek, J. Pfeifer, J. Vogl, H. Traub and B. Meermann, *Anal. Bioanal. Chem.*, 2025, DOI: 10.1007/s00216-025-06064-y.
27 F. Vanhaecke, G. Galbacs, S. Boonen, L. Moens and R. Dams, *J. Anal. At. Spectrom.*, 1995, **10**, 1047–1052.
28 G. J. Puts and P. L. Crouse, *J. Fluorine Chem.*, 2014, **168**, 260–267.
29 F. Vanhaecke, I. Gelaude, L. Moens and R. Dams, *Anal. Chim. Acta*, 1999, **383**, 253–261.
30 F. Vanhaecke, M. Resano, M. Pruneda-Lopez and L. Moens, *Anal. Chem.*, 2002, **74**, 6040–6048.
31 F. Vanhaecke, S. Boonen, L. Moens and R. Dams, *J. Anal. At. Spectrom.*, 1997, **12**, 125–130.